OPTIMAL AND SUBOPTIMAL MMSE PRECODING FOR MULTIUSER MIMO SYSTEMS USING CONSTANT ENVELOPE SIGNALS WITH PHASE QUANTIZATION AT THE TRANSMITTER AND PSK MODULATION

Erico S. P. Lopes and Lukas T. N. Landau

Centre for Telecommunications Studies
Pontifical Catholic University of Rio de Janeiro, Rio de Janeiro, Brazil 22453-900
Email: erico;lukas.landau@cetuc.puc-rio.br

ABSTRACT

We propose an optimal MMSE precoding technique using quantized signals with constant envelope and PSK modulation. Unlike the existing MMSE design for 1-bit resolution, the proposed method employs uniform phase quantization and the bounding step in the branch-and-bound method is different in terms of considering the most restrictive relaxation of the nonconvex problem, which is then utilized for a suboptimal design also. Numerical simulations show that using the MMSE criterion instead of the established maximum distance to decision threshold yields a lower BER in many scenarios and a smaller average number of bound evaluations for low and medium SNR.

***Index Terms*—** Precoding, low-resolution quantization, MIMO systems, branch-and-bound methods, MMSE, constant envelope.

I. INTRODUCTION

Multiuser MIMO systems with large scale antenna arrays are expected to play an important role on the future generations of wireless communication systems [1]. However, a challenge for this technology to overcome is the energy consumption and costs related to the large number of radio front ends. One approach to tackle these issues is the utilization of cheap data converters with low-resolution. Depending on the pathloss, the converters can be one of the most energy consuming elements of a radio front end and since their energy consumption scales exponentially with its resolution in amplitude [2], using a low-resolution in amplitude might be favorable.

Several strategies for precoding with low-resolution data converters exist. Linear precoders such as Phase Zero-forcing (ZF-P) [3] suffer from error floor for medium and high signal-to-noise ratio (SNR). More sophisticated approaches have been presented recently in [4], [5] and [6]. However, [4] and [5] imply rounding and [6] implies the convergence to a local minimum.

Moreover, some optimal precoders exist in literature. In [7] a branch-and-bound algorithm was developed for maximizing the minimum distance to the decision threshold (Max-Min DDT) for the 1-bit case. In addition, in [8] a branch-and-bound algorithm, is presented for finding the transmit vector that minimizes the mean square error (MMSE), also for the 1-bit case. More recently, the study presented in [9] also uses the Max-Min DDT criterion but in contrast to [7] it allows the utilization of PSK modulation and arbitrary phase quantization at the transmitter.

In this study, we propose a novel branch-and-bound algorithm for finding the vector that yields the minimum MSE for uniform phase quantization with arbitrary number of quantization regions in combination with PSK modulation.

In contrast to the Max-Min DDT criterion considered in [5], [7], [9], which is promising in the context of hard decision receivers and the high SNR regime, the used MSE criterion is more general.

Besides the consideration of phase quantization and PSK modulation, the proposed approach uses a different bounding method as the approach presented in [8]. Whereas the approach in [8] employs for relaxation the constant envelope constraint, the presented study relies on the convex hull of the discrete non-convex feasible set, which is by definition the most restrictive relaxation for establishing convexity.

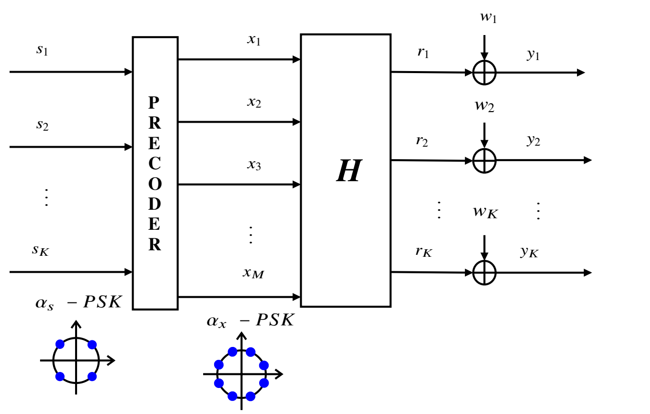

Fig. 1: Multiuser MIMO downlink with phase quantization at the transmitter

Consequently, the lower bounds computed in the present study are greater or equal to the ones computed in [8]. In addition, we propose a suboptimal precoding approach based on the relaxed problem, which we formulate as a convex quadratic program.

The numerical results show that the proposed branch-and-bound method corresponds to a lower uncoded BER in comparison to the state-of-the-art algorithms for the low and intermediate SNR regime.

Moreover, the numerical results confirm that when operating in low SNR, only a small number of bounds needs to be evaluated to determine the optimal solution.

The paper is organized as follows: Section II describes the system model, whereas Section III describes a suboptimal algorithm and an optimal branch-and-bound strategy for the MMSE criterion. Section IV presents and discusses numerical results, while Section V gives the conclusions. A convexity analysis is presented in the appendix.

Regarding the notation, note that real and imaginary part operator are also applied to vectors and matrices, e.g., $\operatorname{Re}\{\boldsymbol{x}\} = [\operatorname{Re}\{[\boldsymbol{x}]_1\}, \ldots, \operatorname{Re}\{[\boldsymbol{x}]_M\}]^T$.

II. SYSTEM MODEL

This study considers a single cell MU-MIMO downlink, where the base station (BS) has full knowledge of the channel state, as shown in Fig. 1. The BS is equipped with M transmitting antennas which serves K single antenna users.

The symbols to be precoded are represented by the data vector $\boldsymbol{s}$ where the i-th entry denotes the data for the i-th user. Every entry of the vector belongs to the set $\mathcal{S}$ which represents all possible symbols of a α_s-PSK modulation and is described by

$$\mathcal{S} = \left\{ s : s = e^{\frac{j\pi(2i+1)}{\alpha_s}}, \text{ for } i = 1, \ldots, \alpha_s \right\}. \tag{1}$$

The data vector $\boldsymbol{s}$ reads as $\boldsymbol{s} = [s_1, \ldots, s_K]^T$, where $\boldsymbol{s} \in \mathcal{S}^K$.

The vector $\boldsymbol{s}$ is then given to the precoder, which computes the transmit vector $\boldsymbol{x} = [x_1, \ldots, x_M]^T$ based on the channel and the noise statistics at the receiver.

The entries of the transmit vector are constrained to the set $\mathcal{X}$, which describes an α_x-PSK alphabet, which is denoted as

$$\mathcal{X} = \left\{ x : x = e^{\frac{j\pi(2i+1)}{\alpha_x}}, \text{ for } i = 1, \ldots, \alpha_x \right\}. \tag{2}$$

The transmit vector $\boldsymbol{x}$ reads $\boldsymbol{x} = [x_1, \ldots, x_K]^T$, where $\boldsymbol{x} \in \mathcal{X}^M$.

Implicitly analog pulse shaping filters are considered at the BS and matched filters are considered at the receivers.

A flat fading channel described by the matrix $\boldsymbol{H}$ with coefficients $h_{k,m}$ is considered, where k and m denote the index of the user and the transmit antenna, respectively.

With this, the noiseless received signals are denoted by

$$r_k = \sum_{m=1}^{M} h_{k,m}\ x_m. \tag{3}$$

In the sequel the symbols are organized using a stacked vector notation in which $\boldsymbol{r} = [r_1, \ldots, r_K]^T$ represents the noiseless received vector.

At the user terminals the received signals are distorted by additive Gaussian noise denoted by the complex random vector $\boldsymbol{w} \sim \mathcal{CN}(0, \boldsymbol{C}_w)$. Using stacked vector notation the received signals at the detectors are denoted by $\boldsymbol{y} = \boldsymbol{H}\boldsymbol{x} + \boldsymbol{w}$.

III. MMSE Precoder Design

In this section we expose the objective of the precoding algorithm, discuss the chosen criterion and propose two new algorithms for low resolution precoding with phase quantization.

The objective of MIMO precoding algorithms is to mitigate the multi-user interference (MUI) and to simultaneously reduce distortions brought by additive noise which can be realized by minimization of the MSE at the receivers. In the case of precoding with low-resolution the problem is more difficult than with full resolution because the transmitting vector is in this case constrained to a discrete set.

Unlike the state-of-the-art discrete precoding algorithm for the MMSE criterion [8], which is devised with 1-bit resolution and uses a constant envelope restriction for the bounding steps, the present study implies arbitrary uniform phase quantization and the consideration of polyhedral constraints like in [9] and similar to [5]. The bounding method based on polyhedra is more promising than the constant envelope formulation, because the corresponding set corresponds to the convex hull and is per definition the smallest convex set that includes all the discrete solutions. Consequently, the corresponding lower bounds are more restricted, such that the bounds can only be larger or equal to the strategy proposed in [8], which is beneficial for reducing candidates when applying a branch-and-bound method and also for finding suboptimal solutions.

A. The Continuous Problem

With a total transmit energy constraint the MMSE problem can be cast as

$$\min_{\boldsymbol{x},f} \mathrm{E}\{\|f\boldsymbol{y} - \boldsymbol{s}\|_2^2\} \quad \text{subject to: } \boldsymbol{x}^H\boldsymbol{x} \leq E_{\mathrm{Tx}}, \quad f > 0. \tag{4}$$

One approach to solve (4) in closed form is based on KKT conditions and the inside that for the optimal precoding vector the transmit energy constraint must hold with equality as described in [10]. Then the optimal precoding vector reads as

$$\boldsymbol{x} = f^{-1}(\boldsymbol{H}^H\boldsymbol{H} + \mathrm{E}\{\boldsymbol{w}^H\boldsymbol{w}\}/E_{\mathrm{Tx}}\boldsymbol{I})^{-1}\boldsymbol{H}^H\boldsymbol{s}, \tag{5}$$

where the optimal scaling factor is given by

$$f = \sqrt{(\boldsymbol{s}^H\boldsymbol{H}(\boldsymbol{H}^H\boldsymbol{H} + \mathrm{E}\{\boldsymbol{w}^H\boldsymbol{w}\}/E_{\mathrm{Tx}}\boldsymbol{I})^{-2}\boldsymbol{H}^H\boldsymbol{s})/E_{\mathrm{Tx}}}. \tag{6}$$

B. Problem for Constant Envelope Signals With Phase Quantization at the Transmitter and PSK Modulation

The problem desribed in (4) considers infinite resolution for the entries in $\boldsymbol{x}$. Considering quantization of the transmit signal yields the restriction to a discrete input alphabet such that the corresponding problem can be cast as

$$\min_{\boldsymbol{x},f} \mathrm{E}\{\|f\boldsymbol{y} - \boldsymbol{s}\|_2^2\} \quad \text{subject to: } \boldsymbol{x} \in \mathcal{X}^M, \quad f > 0. \tag{7}$$

Note that the feasible set is discrete and therefore not convex. In addition, it can be shown that the MMSE objective function in (7) is not jointly convex in $\boldsymbol{x}$ and f as described in the appendix. Accordingly the optimization problem is not convex.

In the sequel, we devise a suboptimal algorithm based on the relaxation of the feasible set and the formulation of an equivalent convex problem. Subsequently, we devise a branch-and-bound strategy for computing the optimal precoding vector.

1) Proposed Mapped Precoder

In this section we propose a suboptimal approach for (7). Since the feasible set of the optimization problem presented by (7) is non convex we replace $\mathcal{X}^M$ by its convex hull $\mathcal{D}$, which is a polyhedron. With this, the problem reads as

$$\min_{\boldsymbol{x},f} \mathrm{E}\{\|f(\boldsymbol{H}\boldsymbol{x} + \boldsymbol{w}) - \boldsymbol{s}\|_2^2\} \quad \text{subject to: } \boldsymbol{x} \in \mathcal{D}, \quad f > 0. \tag{8}$$

Rewriting the problem in a real valued notation yields

$$\min_{\boldsymbol{x}_\mathrm{r},f} \mathrm{E}\{\|f(\boldsymbol{H}_\mathrm{r}\boldsymbol{x}_\mathrm{r} + \boldsymbol{w}_\mathrm{r}) - \boldsymbol{s}_\mathrm{r}\|_2^2\} \quad \text{subject to: } \boldsymbol{A}\boldsymbol{x}_\mathrm{r} \leq \boldsymbol{b}, \quad f > 0, \tag{9}$$

with

$$\boldsymbol{x}_\mathrm{r} = \left[\mathrm{Re}\{\boldsymbol{x}_1\}\ \mathrm{Im}\{\boldsymbol{x}_1\}\ \cdots\ \mathrm{Re}\{\boldsymbol{x}_M\}\ \mathrm{Im}\{\boldsymbol{x}_M\}\right]^T$$

and

$$\boldsymbol{H}_\mathrm{r} = \begin{bmatrix} \mathrm{Re}\{h_{11}\} & -\mathrm{Im}\{h_{11}\} & \cdots & \mathrm{Re}\{h_{1M}\} & -\mathrm{Im}\{h_{1M}\} \\ \mathrm{Im}\{h_{11}\} & \mathrm{Re}\{h_{11}\} & \cdots & \mathrm{Im}\{h_{1M}\} & \mathrm{Re}\{h_{1M}\} \\ \vdots & & \ddots & & \vdots \\ \mathrm{Re}\{h_{K1}\} & -\mathrm{Im}\{h_{K1}\} & \cdots & \mathrm{Re}\{h_{KM}\} & -\mathrm{Im}\{h_{KM}\} \\ \mathrm{Im}\{h_{K1}\} & \mathrm{Re}\{h_{K1}\} & \cdots & \mathrm{Im}\{h_{KM}\} & \mathrm{Re}\{h_{KM}\} \end{bmatrix}.$$

The inequality $\boldsymbol{A}\boldsymbol{x}_\mathrm{r} \leq \boldsymbol{b}$ restricts the elements of the precoding vector to be inside or on the boarder of the polyhedron whose construction will be detailed in the sequel. An equivalent problem to (8) can be cast as

$$\min_{\boldsymbol{x}_\mathrm{r},f} f^2\boldsymbol{x}_\mathrm{r}^T\boldsymbol{H}_\mathrm{r}^T\boldsymbol{H}_\mathrm{r}\boldsymbol{x}_\mathrm{r} - 2f\boldsymbol{x}_\mathrm{r}^T\boldsymbol{H}_\mathrm{r}^T\boldsymbol{s}_\mathrm{r} + f^2\mathrm{E}\{\boldsymbol{w}_\mathrm{r}^T\boldsymbol{w}_\mathrm{r}\} \quad \text{subject to: } \boldsymbol{A}\boldsymbol{x}_\mathrm{r} \leq \boldsymbol{b}, \quad f > 0. \tag{10}$$

If $f \geq 0$ would be constant, the problem would be a convex quadratic program, since $\boldsymbol{H}_\mathrm{r}^T\boldsymbol{H}_\mathrm{r} \in S_+^n$ (cf. Section 4.4 in [11]). Nevertheless, as mentioned before, the problem is in general not jointly convex in f and $\boldsymbol{x}_\mathrm{r}$, as can be seen in the appendix.

Nevertheless, the problem can be transferred into an equivalent convex problem by shifting the scaling factor f to the constraints and a substitution of the optimization variable. In this context, we substitute by introducing a new optimization variable with $\boldsymbol{x}_{\mathrm{r,f}} = f\boldsymbol{x}_\mathrm{r}$. Accordingly, the resulting problem reads as

$$\min_{\boldsymbol{x}_{\mathrm{r,f}},f} \boldsymbol{x}_{\mathrm{r,f}}^T\boldsymbol{H}_\mathrm{r}^T\boldsymbol{H}_\mathrm{r}\boldsymbol{x}_{\mathrm{r,f}} - 2\boldsymbol{x}_{\mathrm{r,f}}^T\boldsymbol{H}_\mathrm{r}^T\boldsymbol{s}_\mathrm{r} + f^2\mathrm{E}\{\boldsymbol{w}_\mathrm{r}^T\boldsymbol{w}_\mathrm{r}\} \quad \text{subject to: } \boldsymbol{A}\boldsymbol{x}_{\mathrm{r,f}} \leq f\boldsymbol{b}, \quad f > 0. \tag{11}$$

The constraint can be rewritten as a linear constraint, such that the problem is denoted by

$$\min_{\boldsymbol{x}_{\mathrm{r,f}},f} \boldsymbol{x}_{\mathrm{r,f}}^T\boldsymbol{H}_{\mathrm{r}}^T\boldsymbol{H}_{\mathrm{r}}\boldsymbol{x}_{\mathrm{r,f}} - 2\boldsymbol{x}_{\mathrm{r,f}}^T\boldsymbol{H}_{\mathrm{r}}^T\boldsymbol{s}_{\mathrm{r}} + f^2\mathrm{E}\{\boldsymbol{w}_{\mathrm{r}}^T\boldsymbol{w}_{\mathrm{r}}\} \quad (12)$$
$$\text{subject to: } [\boldsymbol{A} - \boldsymbol{b}]\begin{bmatrix}\boldsymbol{x}_{\mathrm{r},f}\\ f\end{bmatrix} \leq \boldsymbol{0}, \qquad f > 0,$$

which is a convex quadratic problem (cf. Section 4.4 in [11]). Finally the optimization problem is expressed as

$$\min_{\boldsymbol{x}_{\mathrm{r,f}},f} \boldsymbol{x}_{\mathrm{r,f}}^T\boldsymbol{H}_{\mathrm{r}}^T\boldsymbol{H}_{\mathrm{r}}\boldsymbol{x}_{\mathrm{r,f}} - 2\boldsymbol{x}_{\mathrm{r,f}}^T\boldsymbol{H}_{\mathrm{r}}^T\boldsymbol{s}_{\mathrm{r}} + f^2\mathrm{E}\{\boldsymbol{w}_{\mathrm{r}}^T\boldsymbol{w}_{\mathrm{r}}\} \quad (13)$$
$$\text{subject to: } \boldsymbol{R}\begin{bmatrix}\boldsymbol{x}_{\mathrm{r},f}\\ f\end{bmatrix} \leq \boldsymbol{0}, \qquad f > 0.$$

The polyhedron associated to uniformly phase quantized transmit symbols with α_x different phases can be expressed as proposed before in [9], which is similar to the description in [5]. The corresponding matrix notation reads as

$$\boldsymbol{R} = \left[\boldsymbol{A} - \boldsymbol{b}\right] = \left[\tilde{\boldsymbol{R}}, -\frac{\cos(\frac{\pi}{\alpha_x})}{\sqrt{M}}\boldsymbol{1}_{M\alpha_x}\right], \quad (14)$$

with

$$\tilde{\boldsymbol{R}} = \left[(\boldsymbol{I}_M \otimes \boldsymbol{\beta}_1)^T, (\boldsymbol{I}_M \otimes \boldsymbol{\beta}_2)^T, \ldots, (\boldsymbol{I}_M \otimes \boldsymbol{\beta}_{\alpha_x})^T\right]^T,$$

and

$$\boldsymbol{\beta}_i = \left[\cos\phi_i, -\sin\phi_i\right] \quad \phi_i = \frac{2\pi i}{\alpha_x}, \text{ for } i = 1, \ldots, \alpha_x.$$

Note that the solution of (13) yields a lower bound on the optimal value of the original problem, meaning that the corresponding MSE is smaller or equal to the corresponding MSE of the original problem in (7). Yet, the optimal solution of the relaxed problem is not necessarily in the feasible set of the original problem $\mathcal{X}^M$.

Therefore, in order to find a feasible solution, mapping to the closest Euclidean distance point in $\mathcal{X}^M$ is considered. The solution after mapping, then, yields a MSE which is always greater or equal to the optimal of (7), meaning that after the mapping process an upper bound on the optimal value of the original problem is found.

2) Proposed Optimal Approach via Branch-and-Bound

As stated before, the continuous solution of (13) is in general not in $\mathcal{X}^M$ and then it only provides an unfeasible lower bound, or, after mapping, a feasible upper bound solution for the original problem. In this sense, the method in (13) does not provide a reliable way for solving (7).

Therefore, we propose a branch-and-bound strategy that always provides the optimal solution for (7) with significantly reduced computational complexity as compared to exhaustive search.

In the following we provide explanations of the branch-and-bound concept and then the algorithm is applied to the present precoding problem. The section is divided into four parts, namely Introduction of the Branch-and-Bound Method, Branch-and-Bound Initialization, Subproblems and MMSE Branch-and-Bound Precoding Algorithm.

a) Introduction of the Branch-and-Bound Method

A branch-and-bound algorithm is a tree search based method. The tree represents the set of all possible solutions for the vector $\boldsymbol{x}$, i.e., it is a representation of the set $\mathcal{X}^M$. For the construction of the tree M levels are considered and each node has one ingoing branch and α_x outgoing branches.

For constructing the precoding vector we consider the minimization of an objective function $g(\boldsymbol{x}, \boldsymbol{s})$, which could be the MSE, subject to the feasible discrete set, described by

$$\boldsymbol{x}_{\mathrm{opt}} = \arg\min_{\boldsymbol{x}} g(\boldsymbol{x}, \boldsymbol{s}) \quad \text{s.t. } \boldsymbol{x} \in \mathcal{X}^M. \quad (15)$$

A lower bound on $g(\boldsymbol{x}_{\mathrm{opt}}, \boldsymbol{s})$ can be obtained by relaxing $\mathcal{X}^M$ to its convex hull. The relaxed problem is expressed as

$$\boldsymbol{x}_{\mathrm{lb}} = \arg\min_{\boldsymbol{x}} g(\boldsymbol{x}, \boldsymbol{s}) \quad \text{s.t. } \boldsymbol{x} \in \mathcal{D}. \quad (16)$$

An associated upper bound on $g(\boldsymbol{x}_{\mathrm{opt}}, \boldsymbol{s})$ can be obtained by mapping the solution of (16) and evaluating $g(\cdot)$, as discussed previously on subsection III-B1. The upper bound value of (15) is termed $\breve{g}$.

Having an upper bound solution implies that $\breve{g} \geq g(\boldsymbol{x}_{\mathrm{opt}}) \geq g(\boldsymbol{x}_{\mathrm{lb}})$, which means that the mapped solution is always greater or equal to the relaxed one from (16).

By fixing d entries of $\boldsymbol{x}$, the vector can be rewritten as $\boldsymbol{x} = [\boldsymbol{x}_1^T, \boldsymbol{x}_2^T]^T$, with $\boldsymbol{x}_1 \in \mathcal{X}^d$. With this, a subproblem can be formulated as

$$\boldsymbol{x}_2 = \arg\min_{\boldsymbol{x}_2} g(\boldsymbol{x}_2, \boldsymbol{x}_1, \boldsymbol{s}) \quad (17)$$
$$\text{s.t. } \boldsymbol{x}_2 \in \mathcal{X}^{M-d}.$$

Relaxing the problem from (17) we have

$$\boldsymbol{x}_{2,\mathrm{lb}} = \arg\min_{\boldsymbol{x}_2} g(\boldsymbol{x}_2, \boldsymbol{x}_1, \boldsymbol{s}) \quad (18)$$
$$\text{s.t. } \boldsymbol{x}_2 \in \mathcal{J},$$

where $\mathcal{J}$ is the convex hull of $\mathcal{X}^{M-d}$.

If the optimal value of (18) is larger than a known upper bound $\breve{g}$ on the solution of (15), then all members in the discrete set which include the previously fixed vector $\boldsymbol{x}_1$ can be excluded from the search process.

By this strategy we intend to exclude most of the candidates from the possible solution set, such that the number of residual candidates is only a small fraction of its total number and, thus, they can be evaluated via exhaustive search.

b) Branch-and-Bound Initialization

The branch-and-bound algorithm converges faster when we can compute as early as possible an upper bound that permits many exclusions. Therefore, it is recommended to have an initialization step where an upper-bound $\breve{g} < \infty$ is found before beginning with the search process.

With that in mind, for initialization, the problem described in (13) is solved. This way, $\boldsymbol{x}_{\mathrm{lb}}$ and $g(\boldsymbol{x}_{\mathrm{lb}}) = \mathrm{MSE}_{\mathrm{lb}}$ are obtained. After mapping $\boldsymbol{x}_{\mathrm{ub}}$ and $\breve{g} = \mathrm{MSE}_{\mathrm{ub}}$ are determined.

Note that, if the continuous solution of (13) is in the feasible set, upper and lower bound are equal which can be expressed as

$$\boldsymbol{x}_{\mathrm{ub}} = \boldsymbol{x}_{\mathrm{lb}} = \boldsymbol{x}_{\mathrm{opt}} \rightarrow g(\boldsymbol{x}_{\mathrm{lb}}) = \breve{g}. \quad (19)$$

This would mean that the optimal solution is found already by the approach from subsection III-B1 and the tree search process can be skipped.

c) Subproblems

When the condition from (19) is not met, there is the need to search for the optimal value of $\boldsymbol{x}$. To accomplish this task, it is necessary to solve subproblems, as first mentioned on III-B2a. The equations that define the subproblems are derived below.

First the precoding vector is divided in a fixed vector of length $2d$ and a variable vector according to

$$\boldsymbol{x}_{\mathrm{r}} = \left[\boldsymbol{x}_{\mathrm{r,fixed}}^T, \boldsymbol{x}_{\mathrm{r}}'^T\right]^T. \quad (20)$$

With this, the MMSE problem formulation reads as

$$\min_{\boldsymbol{x}_{\mathrm{r}}', f'} \mathrm{E}\{\|f'(\boldsymbol{H}_{\mathrm{r}}\left[\boldsymbol{x}_{\mathrm{r,fixed}}^T, \boldsymbol{x}_{\mathrm{r}}'^T\right]^T + \boldsymbol{w}_{\mathrm{r}}) - \boldsymbol{s}_{\mathrm{r}}\|_2^2\} \quad (21)$$
$$\text{subject to: } \boldsymbol{A}'\boldsymbol{x}_{\mathrm{r}}' \leq \boldsymbol{b}', \quad f' > 0,$$

where $\boldsymbol{A}'\boldsymbol{x}'_{\mathrm{r}} \leq \boldsymbol{b}'$ restricts the elements of the precoding vector to be inside of the set $\mathcal{J}$ and will be detailed in what follows. The channel can be rewritten accordingly as $\boldsymbol{H}_{\mathrm{r}} = \left[\boldsymbol{H}_{\mathrm{r,\,fixed}}, \boldsymbol{H}_{\mathrm{r}}'\right]$. Then the problem can be cast as

$$\min_{\boldsymbol{x}_{\mathrm{r}}', f'} \mathrm{E}\{\|f'(\boldsymbol{H}_{\mathrm{r}}'\boldsymbol{x}_{\mathrm{r}}' + \boldsymbol{H}_{\mathrm{r,\,fixed}}\boldsymbol{x}_{\mathrm{r,\,fixed}} + \boldsymbol{w}_{\mathrm{r}}) - \boldsymbol{s}_{\mathrm{r}}\|_2^2\} \quad (22)$$
$$\text{subject to: } \boldsymbol{A}'\boldsymbol{x}_{\mathrm{r}}' \leq \boldsymbol{b}', \quad f' > 0,$$

and an equivalent problem is given by

$$\min_{\boldsymbol{x}'_{\mathrm{r}}, f'} \|f'\boldsymbol{H}'_{\mathrm{r}}\ \boldsymbol{x}'_{\mathrm{r}} - \boldsymbol{s}_{\mathrm{r}} + f'\boldsymbol{H}_{\mathrm{r,\ fixed}}\ \boldsymbol{x}_{\mathrm{r,\ fixed}}\|_2^2 + f'^2\mathrm{E}\{\boldsymbol{w}_{\mathrm{r}}^T\boldsymbol{w}_{\mathrm{r}}\} \tag{23}$$
$$\text{subject to: } \boldsymbol{A}'\boldsymbol{x}'_{\mathrm{r}} \le \boldsymbol{b}', \quad f' > 0.$$

The objective function is not jointly convex in f' and $\boldsymbol{x}'_{\mathrm{r}}$, as shown for the conventional MMSE cost function in the appendix.

However, it is possible to shift the scaling factor from the objective in the polyhedron constraint as done in Section III-B1. This essentially means that the feasible set is scaled depending on the value of f'. Accordingly, we substitute the variable with $\boldsymbol{x}'_{\mathrm{r}}\ f' = \boldsymbol{x}'_{\mathrm{r},f}$. Using $\boldsymbol{x}'_{\mathrm{r},f}$, the equivalent problem reads as

$$\min_{\boldsymbol{x}'_{\mathrm{r},f}, f'} \|\boldsymbol{H}'_{\mathrm{r}}\ \boldsymbol{x}'_{\mathrm{r},f} - \boldsymbol{s}_{\mathrm{r}} + f'\boldsymbol{H}_{\mathrm{r,\ fixed}}\ \boldsymbol{x}_{\mathrm{r,\ fixed}}\|_2^2 + f'^2\mathrm{E}\{\boldsymbol{w}_{\mathrm{r}}^T\boldsymbol{w}_{\mathrm{r}}\} \tag{24}$$
$$\text{subject to: } \boldsymbol{A}'\boldsymbol{x}'_{\mathrm{r},f} \le f'\boldsymbol{b}', \quad f' > 0.$$

Rearranging the constraint yields

$$\min_{\boldsymbol{x}'_{\mathrm{r},f}, f'} \|\boldsymbol{H}'_{\mathrm{r}}\ \boldsymbol{x}'_{\mathrm{r},f} - \boldsymbol{s}_{\mathrm{r}} + f'\boldsymbol{H}_{\mathrm{r,\ fixed}}\boldsymbol{x}_{\mathrm{r,\ fixed}}\|_2^2 + f'^2\mathrm{E}\{\boldsymbol{w}_{\mathrm{r}}^T\boldsymbol{w}_{\mathrm{r}}\} \tag{25}$$
$$\text{subject to: } [\boldsymbol{A}' - \boldsymbol{b}'] \begin{bmatrix} \boldsymbol{x}'_{\mathrm{r},f} \\ f' \end{bmatrix} \le \boldsymbol{0}, \quad f' > 0,$$

and finally

$$\min_{\boldsymbol{x}'_{\mathrm{r},f}, f'} \|\boldsymbol{H}'_{\mathrm{r}}\ \boldsymbol{x}'_{\mathrm{r},f} - \boldsymbol{s}_{\mathrm{r}} + f'\boldsymbol{H}_{\mathrm{r,\ fixed}}\ \boldsymbol{x}_{\mathrm{r,\ fixed}}\|_2^2 + f'^2\mathrm{E}\{\boldsymbol{w}_{\mathrm{r}}^T\boldsymbol{w}_{\mathrm{r}}\} \tag{26}$$
$$\text{subject to: } \boldsymbol{R}' \begin{bmatrix} \boldsymbol{x}'_{\mathrm{r},f} \\ f' \end{bmatrix} \le \boldsymbol{0}, \quad f' > 0,$$

where $\boldsymbol{R}'$ is obtained by picking the last $2(M-d)$ columns of $\boldsymbol{R}$ introduced in (14).

Note that the problem in (26) is convex because of the convex constraints and its objective function which is jointly convex in f' and $\boldsymbol{x}'_{\mathrm{r},f}$ as can be seen in the second part of the appendix, where the Hessian is examined.

d) MMSE Branch-and-Bound Precoding Algorithm

In this subsection a branch-and-bound algorithm is proposed which solves (7) with the tools presented in the previous subsections. As mentioned before, the first step is the initialization, where the problem from (13) is solved and the condition $\boldsymbol{x}_{\mathrm{lb}} = \boldsymbol{x}_{\mathrm{ub}}$ is evaluated. If the condition is met, the algorithm returns $\boldsymbol{x}_{\mathrm{lb}}$. Otherwise, there is the need for the tree search process described in the sequel.

For the tree search process a breadth first search is devised and the subproblems are solved with considering partially fixed precoding vectors $\boldsymbol{x}_{\mathrm{r}} = \left[\boldsymbol{x}_{\mathrm{r,fixed}}^T, \boldsymbol{x}_{\mathrm{r}}'^T\right]^T$, where $\boldsymbol{x}_{\mathrm{r,fixed}}$ has length $2d$ as previously stated. Accordingly, the matrices $\boldsymbol{R}$ and $\boldsymbol{H}_{\mathrm{r}}$ are divided as $\boldsymbol{R} = [\boldsymbol{R}_{\mathrm{fixed}}, \boldsymbol{R}']$ and $\boldsymbol{H}_{\mathrm{r}} = \left[\boldsymbol{H}_{\mathrm{r,fixed}}, \boldsymbol{H}'_{\mathrm{r}}\right]$, where $\boldsymbol{R}_{\mathrm{fixed}}$ and $\boldsymbol{H}_{\mathrm{r,fixed}}$ contains the first $2d$ columns of $\boldsymbol{R}$ and $\boldsymbol{H}_{\mathrm{r}}$.

Using $\boldsymbol{R}'$ and $\boldsymbol{H}'_{\mathrm{r}}$, the subproblem (26) for the lower-bounding step is solved. Mapping the solution from (26) to the discrete set yields $\boldsymbol{x}_{\mathrm{r,ub}}$. Based on $\boldsymbol{x}_{\mathrm{r,ub}}$, the MSE is minimized with choosing

$$f' = \frac{\boldsymbol{s}_{\mathrm{r}}^T\boldsymbol{H}_{\mathrm{r}}\begin{bmatrix}\boldsymbol{x}_{\mathrm{r,fixed}} \\ \boldsymbol{x}_{\mathrm{r,ub}}\end{bmatrix}}{\left\|\boldsymbol{H}_{\mathrm{r}}\begin{bmatrix}\boldsymbol{x}_{\mathrm{r,fixed}} \\ \boldsymbol{x}_{\mathrm{r,ub}}\end{bmatrix}\right\|_2^2 + \mathrm{E}\{\boldsymbol{w}_{\mathrm{r}}^T\boldsymbol{w}_{\mathrm{r}}\}}. \tag{27}$$

The corresponding MSE serves as an upper bound on the optimal value of the original problem ($\mathrm{MSE}_{\mathrm{ub}}$).

In case the lower bound conditioned on $\boldsymbol{x}_{\mathrm{r,fixed}}$ is higher than any upper bound on the original problem, $\boldsymbol{x}_{\mathrm{r,fixed}}$ cannot be part of the solution and every member of the discrete solution set which includes $\boldsymbol{x}_{\mathrm{r,fixed}}$ can be excluded from the search process. The steps of the method are detailed in Algorithm 1.

Algorithm 1 Proposed B&B Precoding for solving (7)

initialization:
Given the channel $\boldsymbol{H}$ and transmit symbols $\boldsymbol{s}$ compute a valid upper bound $\breve{g}$ on the problem in (7), by solving (13) followed by a mapping to the closest precoding vector $\boldsymbol{x} \in \mathcal{X}^M$ and computing its MSE. If the solution of (13) belongs to $\mathcal{X}^M$ it is the optimal. Otherwise,

define the first level ($d = 1$) of the tree by $\mathcal{G}_d := \mathcal{X}$

for $d = 1 : M-1$ **do**
  Partition $\mathcal{G}_d$ in $\boldsymbol{x}_{\mathrm{fixed},1}, \ldots, \boldsymbol{x}_{\mathrm{fixed},|\mathcal{G}_d|}$
  for $i = 1 : |\mathcal{G}_d|$ **do**
    Express $\boldsymbol{x}_{\mathrm{fixed},i}$ in real valued notation $\boldsymbol{x}_{\mathrm{r,fixed},i}$
    Conditioned on $\boldsymbol{x}_{\mathrm{r,fixed},i}$ solve (26) to find $\boldsymbol{x}'_{\mathrm{r},f}$ and f'
    Determine the lower bound $\mathrm{MSE}_{\mathrm{lb}} :=$
    $\|\boldsymbol{H}'_{\mathrm{r}}\ \boldsymbol{x}'_{\mathrm{r},f} - \boldsymbol{s}_{\mathrm{r}} + f'\boldsymbol{H}_{\mathrm{r,\ fixed}}\boldsymbol{x}_{\mathrm{r,\ fixed,i}}\|_2^2 + f'^2\mathrm{E}\{\boldsymbol{w}_{\mathrm{r}}^T\boldsymbol{w}_{\mathrm{r}}\}$
    Extract $\boldsymbol{x}'_{\mathrm{r}} = \frac{\boldsymbol{x}'_{r,f}}{f'}$
    Rewrite $\boldsymbol{x}'_{\mathrm{r}}$ in complex notation as $\boldsymbol{x}'_{\mathrm{lb}}$
    Map $\boldsymbol{x}'_{\mathrm{lb}}$ to the discrete solution with the closest Euclidean distance: $\boldsymbol{x}'_{\mathrm{ub}}(\boldsymbol{x}'_{\mathrm{lb}}) \in \mathcal{X}^{M-d}$
    Express $\boldsymbol{x}'_{\mathrm{ub}}$ in real valued notation $\boldsymbol{x}'_{\mathrm{r,ub}}$
    Compute f' according to (27)
    With $\boldsymbol{x}'_{\mathrm{r,ub}}$ and f', the upper bound is $\mathrm{MSE}_{\mathrm{ub}}(\boldsymbol{x}_{\mathrm{r,fixed,i}}) :=$
    $$\left\| f'\boldsymbol{H}_{\mathrm{r}}\begin{bmatrix}\boldsymbol{x}_{\mathrm{r,fixed,i}} \\ \boldsymbol{x}'_{\mathrm{r,ub}}\end{bmatrix} - \boldsymbol{s}_{\mathrm{r}}\right\|_2^2 + f'^2\mathrm{E}\{\boldsymbol{w}_{\mathrm{r}}^T\boldsymbol{w}_{\mathrm{r}}\}$$
    Update the best upper bound with:
    $\breve{g} = \min(\breve{g}, \mathrm{MSE}_{\mathrm{ub}})$
  end for
  Construct a reduced set by comparing conditioned lower bounds with the global upper bound $\breve{g}$
  $\mathcal{G}'_d := \left\{\boldsymbol{x}'_{\mathrm{lb},i} | \mathrm{MSE}_{\mathrm{lb}}(\boldsymbol{x}'_{\mathrm{lb},i}) \le \breve{g}, i = 1, \ldots, |\mathcal{G}_d|\right\}$
  Define the set for the next level in the tree: $\mathcal{G}_{d+1} := \mathcal{G}'_d \times \mathcal{X}$
end for

Search method for the ultimate level $d = M$,

Partition $\mathcal{G}_1$ in $\boldsymbol{x}_{\mathrm{fixed},1}, \ldots, \boldsymbol{x}_{\mathrm{fixed},|\mathcal{G}_1|}$
Express $\boldsymbol{x}_{\mathrm{fixed},i}$ with real valued notation $\boldsymbol{x}_{\mathrm{r,fixed},i}$ and compute f' with (27)

$$\mathrm{MSE}(\boldsymbol{x}_{\mathrm{fixed},i}) := \left\| f'\boldsymbol{H}_{\mathrm{r}}\ \boldsymbol{x}_{\mathrm{r,fixed,i}} - \boldsymbol{s}_{\mathrm{r}}\right\|_2^2 + f'^2\mathrm{E}\{\boldsymbol{w}_{\mathrm{r}}^T\boldsymbol{w}_{\mathrm{r}}\}$$

The global solution is :
$$\boldsymbol{x}_{\mathrm{opt}} = \arg\min_{\boldsymbol{x}_{\mathrm{fixed},i} \in \mathcal{G}_1} \mathrm{MSE}(\boldsymbol{x}_{\mathrm{fixed},i})$$

IV. Numerical Results

In what follows, the proposed methods are compared with the state-of-the-art algorithms in terms of uncoded BER, where Gray-coding is employed. The channel matrix coefficients are considered to be i.i.d. with $h_{k,m} \sim \mathcal{CN}(0, \sigma_h^2)$, and the noise samples are complex Gaussian random variables with $\boldsymbol{w} \sim \mathcal{CN}(0, \sigma_w^2\boldsymbol{I})$. The SNR is defined by $\mathrm{SNR} = \frac{\|\boldsymbol{x}\|_2^2}{\sigma_w^2}$. All numerical computations rely on 100 random channel realizations.

The proposed methods are compared with the following state-of-the-art precoding algorithms:

1. The MSM-Precoder [5], which corresponds to solving an LP with computational complexity in the order of $\mathcal{O}((2M+1)^{3.5})$, when using interior point methods (IPM)

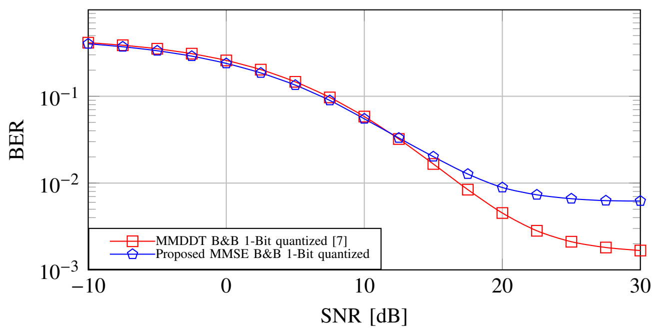

Fig. 2: Uncoded BER versus SNR, $K = 2$, $M = 4$, $\alpha_s = 4$ and $\alpha_x = 4$

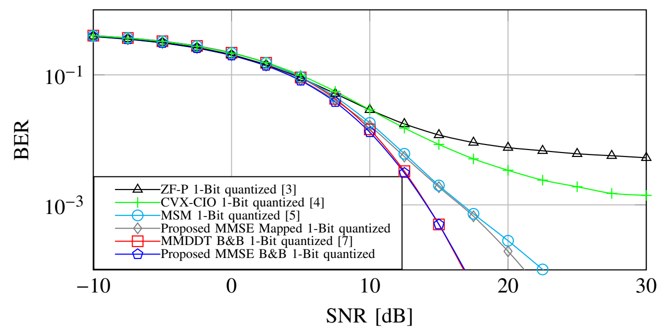

Fig. 3: Uncoded BER versus SNR, $K = 3$, $M = 12$, $\alpha_s = 4$ and $\alpha_x = 4$

2. The Phase Zero-forcing precoder with constant envelope [3] with $O(K^2M)$, whose precoding vectors are subsequently phase quantized
3. The CIO precoder implemented via CVX [4], which corresponds to solving a second order cone program with $O((2M+1)^{3.5})$, when using IPM
4. The MMDDT B&B precoder [9] in which the sub problems correspond to solving a LP with $O((2M+1)^{3.5})$, when using IPM

A. 1-bit DAC

In this subsection we evaluate the performance of the proposed algorithms with 1-bit quantization. In this case, both, the data and the transmit vector symbols are QPSK, which means $\alpha_s = 4$ and $\alpha_x = 4$.

Two different scenarios are considered. First, we compare only the BER performance of the proposed branch-and-bound approach with the algorithm developed in [7], for $K = 2$ users and $M = 4$ antennas at the BS. The BER performances are illustrated in Fig. 2.

Then we consider $K = 3$ users and the number of antennas at the BS $M = 12$ and compare both proposed methods with state-of-the-art approaches. The BER performances are illustrated in Fig. 3. Moreover, the computational complexity in terms of the average number of evaluated bounds is shown in Fig. 4.

Fig. 2 confirms the superiority of the MMSE criterion against MMDDT for low SNR. However, for high SNR, the MMDDT criterion is asymptotically optimal in the sense of BER and yields, as expected, a lower BER.

The results shown in Fig. 3 illustrate a significant gain in BER when using the optimal branch-and-bound method in comparison to suboptimal methods. Moreover, Fig. 3 confirms the suitability of the MMSE criterion for low SNR. Besides that, the results indicate that the proposed suboptimal approach termed MMSE Mapped surprisingly outperforms other suboptimal state-of-the-art algorithms in terms of BER performance.

Moreover, Fig. 4 shows that the number of evaluated bounds of the proposed B&B method is significantly smaller than the one from [7] for low SNR, which underlines the superiority of our proposed method to the existing ones for low SNR.

By using IPM, the subproblems can be solved with a computational complexity in the order of $O(n^{3.5})$, with $n \leq (2M+1)$, cf. [11]. Based on Fig. 4, the average number of subproblems is always significantly smaller than the total number of candidates to be evaluated in the exhaustive search. Taking into account that each candidate evaluation in the exhaustive search corresponds to a complexity of $O(K^2M)$ justifies the utilization of the proposed method when the optimal precoding vector is desired.

B. Phase Quantization

In this subsection the performance of the proposed algorithms with phase quantization is evaluated. In that case, both, the data and the transmit symbol alphabet are considered to be 8-PSK, meaning $\alpha_s = 8$

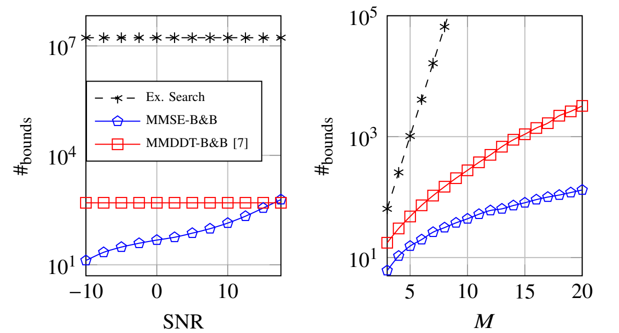

Fig. 4: Average # of evaluated bounds × SNR, $K = 3$, $M = 12$ dB (left). Average # of evaluated bounds × Number of transmit antennas, $K = 3$, SNR = 3 dB (right)

and $\alpha_x = 8$. We consider $K = 2$ users and the number of antennas at the BS is $M = 6$. The corresponding BER performances are illustrated in Fig. 5.

As expected, the proposed branch-and-bound algorithm shows a significantly lower BER than existing suboptimal algorithms and surpasses the optimal precoder with the MMDDT criterion [9] for low SNR as for the 1-bit case. Moreover, surprisingly the proposed mapped precoder yields a slightly lower BER than the existing suboptimal algorithm presented in [5], which relies on the MMDDT criterion.

V. Conclusions

Two precoding algorithms based on the MMSE criterion for phase quantization and PSK modulation were proposed. The first algorithm provides a suboptimal solution and the second computes the optimal solution via branch-and-bound method. The proposed optimal algorithm outperforms the state-of-the-art techniques for this class of precoding in terms of uncoded BER for low and medium SNR values. Numerical results confirm the efficiency of the proposed branch-and-bound strategy.

Appendix - Convexity Analysis

The Conventional MMSE Cost Function With the Scaling Factor

The corresponding real valued function of the equivalent MMSE cost function including the scaling factor reads as

$$J(\boldsymbol{x}_\mathrm{r}, f) = f^2 \boldsymbol{x}_\mathrm{r}^T \boldsymbol{H}_\mathrm{r}^T \boldsymbol{H}_\mathrm{r} \boldsymbol{x}_\mathrm{r} - 2f \boldsymbol{x}_\mathrm{r}^T \boldsymbol{H}_\mathrm{r}^T \boldsymbol{s}_\mathrm{r} + f^2 \mathrm{E}\{\boldsymbol{w}_\mathrm{r}^T \boldsymbol{w}_\mathrm{r}\}. \qquad (28)$$

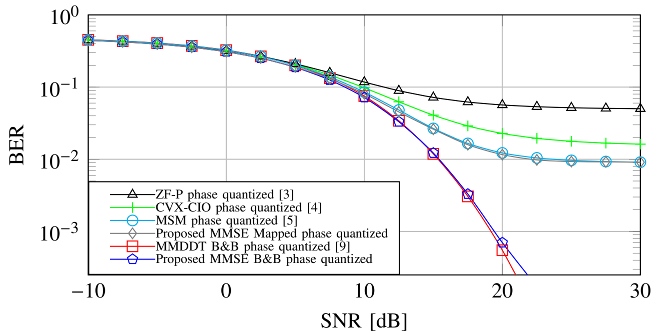

Fig. 5: Uncoded BER versus SNR, $K = 2$, $M = 6$, $\alpha_s = 8$ and $\alpha_x = 8$

The Hessian is constructed based on the partial derivatives given by

$$\begin{aligned} \boldsymbol{\Gamma} &= \frac{\partial^2 J(\boldsymbol{x}_\mathrm{r}, f)}{\partial \boldsymbol{x}_\mathrm{r} \partial \boldsymbol{x}_\mathrm{r}^T} = 2f^2 \boldsymbol{H}_\mathrm{r}^T \boldsymbol{H}_\mathrm{r}, \\ \epsilon &= \frac{\partial^2 J(\boldsymbol{x}_\mathrm{r}, f)}{\partial f^2} = 2\|\boldsymbol{H}_\mathrm{r}\boldsymbol{x}_\mathrm{r}\|_2^2 + 2\mathrm{E}\{\boldsymbol{w}_\mathrm{r}^T \boldsymbol{w}_\mathrm{r}\} \geq 0, \\ \boldsymbol{\eta} &= \frac{\partial^2 J(\boldsymbol{x}, f)}{\partial \boldsymbol{x}_\mathrm{r} \partial f} = 4f \boldsymbol{H}_\mathrm{r}^T \boldsymbol{H}_\mathrm{r} \boldsymbol{x}_\mathrm{r} - 2\boldsymbol{H}_\mathrm{r}^T \boldsymbol{s}_\mathrm{r}. \end{aligned} \tag{29}$$

Positive semi-definiteness of the Hessian is established when the following inequality holds

$$\boldsymbol{v}^T \boldsymbol{\Gamma} \boldsymbol{v} + \nu^2 \epsilon + 2\nu \boldsymbol{\eta}^T \boldsymbol{v} \geq 0 \quad \text{for all } \nu, \boldsymbol{v}. \tag{30}$$

Assuming that $\boldsymbol{\Gamma} \succ \boldsymbol{0}$, the minimum value of (30) is given by $\nu^2 \epsilon - \nu^2 \boldsymbol{\eta}^T \boldsymbol{\Gamma}^{-1} \boldsymbol{\eta}$. For Positive semi-definiteness the minimum cannot be smaller than zero which yields the condition

$$\epsilon \geq \boldsymbol{\eta}^T \boldsymbol{\Gamma}^{-1} \boldsymbol{\eta}. \tag{31}$$

Inserting the partial derivatives gives

$$2\|\boldsymbol{H}_\mathrm{r}\boldsymbol{x}_\mathrm{r}\|_2^2 + 2\mathrm{E}\{\boldsymbol{w}_\mathrm{r}^T \boldsymbol{w}_\mathrm{r}\} \geq \frac{1}{2f^2} \boldsymbol{\eta}^T (\boldsymbol{H}_\mathrm{r}^T \boldsymbol{H}_\mathrm{r})^{-1} \boldsymbol{\eta}, \tag{32}$$

$$\begin{aligned} &2\|\boldsymbol{H}_\mathrm{r}\boldsymbol{x}_\mathrm{r}\|_2^2 + 2\mathrm{E}\{\boldsymbol{w}_\mathrm{r}^T \boldsymbol{w}_\mathrm{r}\} \geq \\ &8\boldsymbol{x}_\mathrm{r}^T \boldsymbol{H}_\mathrm{r}^T \boldsymbol{H}_\mathrm{r} \boldsymbol{x}_\mathrm{r} - \frac{8}{f} \boldsymbol{x}_\mathrm{r}^T \boldsymbol{H}_\mathrm{r}^T \boldsymbol{s}_\mathrm{r} + 2\boldsymbol{s}_\mathrm{r}^T \boldsymbol{H}_\mathrm{r} (\boldsymbol{H}_\mathrm{r}^T \boldsymbol{H}_\mathrm{r})^{-1} \boldsymbol{H}_\mathrm{r}^T \boldsymbol{s}_\mathrm{r}, \end{aligned} \tag{33}$$

which can be rearranged as

$$\frac{8}{f} \boldsymbol{x}_\mathrm{r}^T \boldsymbol{H}_\mathrm{r}^T \boldsymbol{s}_\mathrm{r} \geq 6\boldsymbol{x}_\mathrm{r}^T \boldsymbol{H}_\mathrm{r}^T \boldsymbol{H}_\mathrm{r} \boldsymbol{x}_\mathrm{r} + 2\boldsymbol{s}_\mathrm{r}^T \boldsymbol{H}_\mathrm{r} (\boldsymbol{H}_\mathrm{r}^T \boldsymbol{H}_\mathrm{r})^{-1} \boldsymbol{H}_\mathrm{r}^T \boldsymbol{s}_\mathrm{r} - 2\mathrm{E}\{\boldsymbol{w}_\mathrm{r}^T \boldsymbol{w}_\mathrm{r}\}.$$

We conclude that the MMSE cost function is in general not jointly convex in $\boldsymbol{x}_\mathrm{r}$ and f.

The Partial MMSE Cost Function

The MMSE cost function for the problem formulation with the f' scaled polyhedron and partially fixed precoding vector is given by

$$J\left(\boldsymbol{x}'_{\mathrm{r},f}, f'\right) = \left\| \boldsymbol{H}'_\mathrm{r} \boldsymbol{x}'_{\mathrm{r},f} - \boldsymbol{s}_\mathrm{r} + f' \boldsymbol{H}_{\mathrm{r,\,fixed}} \boldsymbol{x}_{\mathrm{r,\,fixed}} \right\|_2^2 + f'^2 \mathrm{E}\{\boldsymbol{w}_\mathrm{r}^T \boldsymbol{w}_\mathrm{r}\}. \tag{34}$$

As in the previous subsection the Hessian can be constructed with the partial derivatives which are now given by

$$\begin{aligned} \boldsymbol{\Gamma} &= \frac{\partial^2 J(\boldsymbol{x}'_{\mathrm{r},f}, f')}{\partial \boldsymbol{x}'_{\mathrm{r},f} \partial \boldsymbol{x}'^T_{\mathrm{r},f}} = 2\boldsymbol{H}'^T_\mathrm{r} \boldsymbol{H}'_\mathrm{r}, \\ \epsilon &= \frac{\partial^2 J(\boldsymbol{x}'_{\mathrm{r},f}, f')}{\partial f'^{\,2}} = 2\|\boldsymbol{H}_{\mathrm{r,\,fixed}} \boldsymbol{x}_{\mathrm{r,\,fixed}})\|_2^2 + 2\mathrm{E}\{\boldsymbol{w}_\mathrm{r}^T \boldsymbol{w}_\mathrm{r}\} \geq 0, \\ \boldsymbol{\eta} &= \frac{\partial^2 J(\boldsymbol{x}'_{\mathrm{r},f}, f')}{\partial \boldsymbol{x}'_{\mathrm{r},f} \partial f'} = 2\boldsymbol{H}'^T_\mathrm{r} \boldsymbol{H}_{\mathrm{r,\,fixed}} \boldsymbol{x}_{\mathrm{r,\,fixed}}. \end{aligned} \tag{35}$$

Analogous to the previous subsection we assume that $\boldsymbol{\Gamma} \succ \boldsymbol{0}$ and then (31) is a sufficient condition for convexity. In this case, (31), after including the partial derivatives (35), can be rearranged to

$$\mathrm{E}\{\boldsymbol{w}_\mathrm{r}^T \boldsymbol{w}_\mathrm{r}\} \geq \boldsymbol{x}_{\mathrm{r,\,fixed}}^T \boldsymbol{H}_{\mathrm{r,\,fixed}}^T (\boldsymbol{H}'_\mathrm{r} (\boldsymbol{H}'^T_\mathrm{r} \boldsymbol{H}'_\mathrm{r})^{-1} \boldsymbol{H}'^T_\mathrm{r} - \boldsymbol{I}) \boldsymbol{H}_{\mathrm{r,\,fixed}} \boldsymbol{x}_{\mathrm{r,\,fixed}}. \tag{36}$$

Convexity is established by showing that the RHS of (36) is always smaller or equal to zero. This can be shown by considering

$$\boldsymbol{v}^T (\boldsymbol{H}'_\mathrm{r} (\boldsymbol{H}'^T_\mathrm{r} \boldsymbol{H}'_\mathrm{r})^{-1} \boldsymbol{H}'^T_\mathrm{r} - \boldsymbol{I}) \boldsymbol{v} \leq 0, \tag{37}$$

which holds for all $\boldsymbol{v}$, since $\boldsymbol{H}'_\mathrm{r} (\boldsymbol{H}'^T_\mathrm{r} \boldsymbol{H}'_\mathrm{r})^{-1} \boldsymbol{H}'^T_\mathrm{r}$ is a projection matrix where the eigenvalues can only be one or zero.

Acknowledgements

This work has been supported in part by the ELIOT ANR-18-CE40-0030 and FAPESP 2018/12579-7 project and the CNPq Universal 438043/2018-9 project.

VI. References

[1] F. Boccardi, R. W. Heath, A. Lozano, T. L. Marzetta, and P. Popovski, “Five disruptive technology directions for 5G,” *IEEE Commun. Mag.*, vol. 52, no. 2, pp. 74–80, February 2014.

[2] R.H. Walden, “Analog-to-digital converter survey and analysis,” *IEEE J. Sel. Areas Commun.*, vol. 17, no. 4, pp. 539 –550, Apr. 1999.

[3] S. K. Mohammed and E. G. Larsson, “Per-antenna constant envelope precoding for large multi-user MIMO systems,” *IEEE Trans. Commun.*, vol. 61, no. 3, pp. 1059–1071, March 2013.

[4] P. V. Amadori and C. Masouros, “Constant envelope precoding by interference exploitation in phase shift keying-modulated multiuser transmission,” *IEEE Trans. Commun.*, vol. 16, no. 1, pp. 538–550, Jan 2017.

[5] H. Jedda, A. Mezghani, A. L. Swindlehurst, and J. A. Nossek, “Quantized constant envelope precoding with PSK and QAM signaling,” *IEEE Trans. Wireless Commun.*, vol. 17, no. 12, pp. 8022–8034, Dec 2018.

[6] A. Nedelcu, F. Steiner, M. Staudacher, G. Kramer, W. Zirwas, R. S. Ganesan, P. Baracca, and S. Wesemann, “Quantized precoding for multi-antenna downlink channels with MAGIQ,” in *Proc. of the 22nd Int. ITG Workshop on Smart Antennas*, Bochum, Germany, March 2018.

[7] L. T. N. Landau and R. C. de Lamare, “Branch-and-bound precoding for multiuser MIMO systems with 1-bit quantization,” *IEEE Wireless Commun. Lett.*, vol. 6, no. 6, pp. 770–773, Dec 2017.

[8] S. Jacobsson, W. Xu, G. Durisi, and C. Studer, “MSE-optimal 1-bit precoding for multiuser MIMO via branch and bound,” in *Proc. IEEE Int. Conf. Acoust., Speech, Signal Process.*, Calgary, Alberta, Canada, April 2018, pp. 3589–3593.

[9] E. S. P. Lopes and L. T. N. Landau, “Optimal precoding for multiuser MIMO systems with phase quantization and PSK modulation via branch-and-bound,” *arXiv e-prints*, p. arXiv:1909.12442, Sep 2019.

[10] M. Joham, W. Utschick, and J. A. Nossek, “Linear transmit processing in MIMO communications systems,” *IEEE Trans. Signal Process.*, vol. 53, no. 8, pp. 2700–2712, Aug 2005.

[11] S. Boyd and L. Vandenberghe, *Convex Optimization*, Cambridge University Press, New York, NY, USA, 2004.